

AN EXPERIMENTAL INVESTIGATION OF THERMAL
NOISE OF A SILICON CUBE LAW
DOUBLE-INJECTION DIODE

By

JOHN ALAN MAXWELL
//

Bachelor of Science

Oklahoma State University

Stillwater, Oklahoma

1971

Submitted to the Faculty of the Graduate College
of the Oklahoma State University
in partial fulfillment of the requirements
for the Degree of
MASTER OF SCIENCE
May, 1973

JUN 1 1973

AN EXPERIMENTAL INVESTIGATION OF THERMAL
NOISE OF A SILICON CUBE LAW
DOUBLE-INJECTION DIODE

Thesis Approved:

J. R. Bigel

Thesis Adviser

Bennett Basore

T. J. Alvin

D. Durham

Dean of the Graduate College

ACKNOWLEDGMENTS

I wish to express my sincere thanks to Professor Hans R. Bilger for the research problem and his constant advice and help, especially in the dark moments of this work.

I also wish to thank Professor Bennett Basore and Professor Harold Fristoe for serving on my committee.

A special thanks goes to Mr. Sam Weaver at Texas Instruments for supplying the low noise FET used in the preamplifier.

Finally, to my wife, Norma, I express my warmest appreciation for her encouragement and sacrifice during this last semester.

TABLE OF CONTENTS

Chapter	Page
I. INTRODUCTION	1
The Problem	1
II. EXPERIMENTAL APPARATUS	2
The Apparatus	2
Preamplifier and Input Circuitry	2
Input Circuitry	9
Noise Calibration	9
III. EXPERIMENTAL RESULTS	11
Background	11
Results	12
Computer Evaluation of the Data	12
IV. ERROR ANALYSIS	17
Statistical Errors	17
Equipment Errors	18
Linearity Checks	19
Resistor Calibration	21
V. CONCLUSIONS	25
Recommendations for Further Study	25
BIBLIOGRAPHY	26

LIST OF TABLES

Table	Page
I. The Fitted Values of I_{eqth} , b and n	15
II. I_{eqth} and $I_{eqr_{f \rightarrow \infty}}$	16
III. Integrator Gain	20
IV. Expected and Measured Values of I_{eqR}	23

LIST OF FIGURES

Figure	Page
1. Noise Analyzer Layout	3
2. Equivalent Noise Resistance of the Preamplifier	6
3. Preamplifier, Noise Calibration Tube, and DID Bias	7
4. Voltage Gain in (db) of the Preamplifier vs. Frequency	8
5. Equivalent Circuit for a DID	11
6. The I-V Characteristics of Diode 2.8	13
7. Measured Noise Spectra for Device 2.8	14
8. V_m^2 vs I_c at 1MHz	21
9. V_m^2 vs I_c at 22MHz	22
10. Noise Spectra for Three Resistors, 100Ω , 1000Ω and $10,000\Omega$	24

LIST OF SYMBOLS

α	Relative Standard Error	
f	Frequency	(Hz)
Δf	Frequency Bandwidth	(Hz)
I	Device D-C Current	(μA)
I_c	Noise Calibrator Diode D-C Current	(μA)
I_{eq}	Equivalent Noise Current of the Sample	(μA)
I_{eqR}	Equivalent Noise Current of a Resistor	(μA)
I_{eqth}	Equivalent Thermal Noise Current of the Device	
	Calculated From Computer Program	(μA)
I_{eqz}	Equivalent Noise Current of the Preamplifier Input	(μA)
K	Boltzmann's Constant 1.38×10^{-23}	$\frac{\text{V} \cdot \text{A} \cdot \text{s}}{\text{K}}$
L_1	Low Frequency Equivalent Inductance (τ_r)	$\text{V} \cdot \text{s} / \text{A}$
q	Charge of an Electron 1.60×10^{-19}	(As)
R	Resistance	(Ω)
$r_{f \rightarrow \infty}$	Equivalent Device Resistance at Large Frequencies	(Ω)
r_1	Low Frequency Equivalent Resistance of the Device	(Ω)
T	Temperature	(K)
t	Integration Time	(s)
τ	Carrier Lifetime	(s)

CHAPTER I

INTRODUCTION

The Problem

Lee (2) demonstrated that the noise of a double-injection diode (DID) consists of a thermal noise component and a frequency dependent component. The experimental investigation consisted of obtaining by laboratory measurement the thermal component of the noise of the double-injection diode under various D-C operating conditions in a frequency range of 10KHz to 22MHz.

Before noise spectra could be measured, a preamplifier with a very high input impedance, very low internal noise, wider bandwidth and an internal noise calibration source had to be designed and constructed. Once the preamplifier was constructed, noise spectra of the device were obtained experimentally.

CHAPTER II

EXPERIMENTAL APPARATUS

The Apparatus

To make noise measurements, a noise analyzer is needed. This analyzer consisted of a preamplifier, a noise calibration source, a wave analyzer for noise detection and frequency selectivity, various biasing power supplies and an integrator for averaging the wave analyzer output. Figure 1 shows the noise analyzer layout.

The oscilloscope was used to monitor the output of the preamplifier so any spurious oscillations could be detected. The wave analyzer was used as a tunable filter to investigate the noise over the frequency range of 10KHz to 22MHz. The wave analyzer output was integrated to smooth the fluctuations. A digital voltmeter was used to get readings of the integrator output. The various power supplies supply the proper biasing for the preamplifier, noise calibration and bias for the DID.

Preamplifier and Input Circuitry

The preamplifier had to have sufficient gain and low noise to amplify the noise of a 50Ω resistor so it could be detected by the wave analyzer using the $10\mu\text{V}$ input sensitivity setting. Van der Ziel (1) shows by Nyquist's Theorem that the thermal noise for a resistor is given by

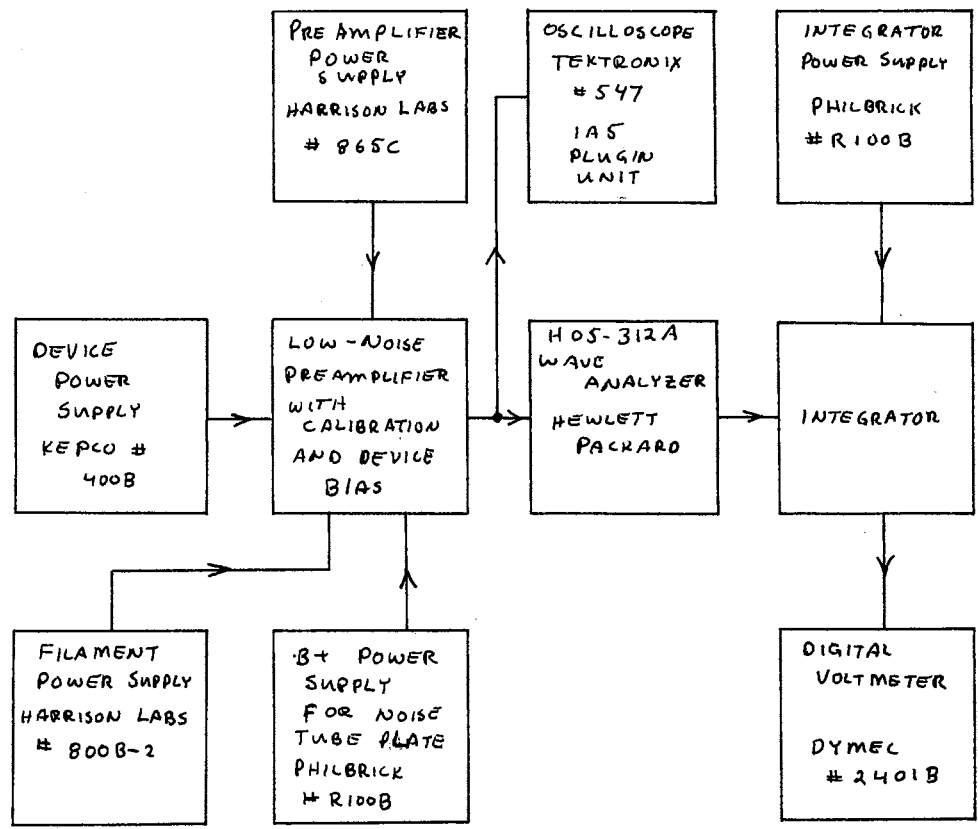


Figure 1. Noise Analyzer Layout

$$\overline{V^2} = 4KTR\Delta f \quad 2.1$$

where

K = Boltzmann's Constant

T = Temperature in degrees Kelvin

Δf = Bandwidth in hertz

R = Resistance in ohms

$$\sqrt{\overline{V^2}} = V_{\text{RMS}} = [4KTR\Delta f]^{1/2} \quad 2.2$$

For $R = 50\Omega$, $T = 300^\circ\text{K}$, and $\Delta f = 3000\text{ Hz}$

$$V_{\text{RMS}} \approx 51\text{ nV}$$

A design goal was that the preamplifier should be sensitive enough to detect the noise of a 50Ω resistor, or the equivalent input noise of the preamplifier should be of the same magnitude of a 50Ω resistor's noise.

The preamplifier must also be able to match a very large source impedance variation without increasing the preamplifier's contribution to the total noise. The device impedance will vary from a few hundred ohms to many thousand ohms. Because of the wide variation of source impedance, a low noise Field Effect Transistor (FET) was used in the preamplifier input stage in order to utilize its high input impedance.

The equivalent input noise voltage can be represented as an equivalent input noise resistance. Van der Ziel (3) has shown that the equivalent noise resistance of a junction FET is given by

$$R_{\text{eq}} = Q/g_m \quad 2.3$$

where g_m is the transconductance of the FET and $Q \approx 2/3$. A SFB8558 low noise FET was used in the input stage of the preamplifier. This particular transistor had a $g_m = 17\text{mA/V}$ at $V_{\text{GS}} = 0\text{V}$, which corresponds to

an expected value of R_{eq} of approximately 40Ω . Figure 2 shows that the measured value of R_{eq} equals approximately 53Ω which is sufficiently close to the expected value of 40Ω .

Lee (2) showed that for the HOS-312A wave analyzer detector, the true RMS noise voltage is given by

$$V_{RMS} = \frac{2}{\sqrt{\pi}} V_{indicated} \quad 2.4$$

An arbitrary requirement was set that the noise of a 50Ω resistor should be indicated by a midscale reading on the $10\mu V$ setting of the wave analyzer with a bandwidth of 3000 Hz. (A $5\mu V$ reading corresponds to a true RMS value of $5.65\mu V$.)

The necessary voltage gain of the preamplifier can be found by dividing the true RMS value of an indicated $5\mu V$ by the RMS noise voltage of a 50Ω resistor.

$$A_V = 110 \quad (40.8 \text{ db}) \quad 2.5$$

There is some leeway in the necessary voltage gain because the wave analyzer has a more sensitive scale setting.

A FET-Bipolar transistor cascode amplifier was used for the input stage driving a Bipolar-Bipolar transistor cascode amplifier for additional gain. The second cascode amplifier drives a Darlington common emitter amplifier cable driver. This type of cable driver was chosen after experimenting with different types of emitter followers. The input of the wave analyzer was terminated with 50Ω to minimize capacitive loading of the cable driver.

Figure 3 shows the preamplifier schematic with the noise calibration and the DID biasing at the input. Figure 4 shows the voltage gain of the preamplifier which meets the desired gain requirement.

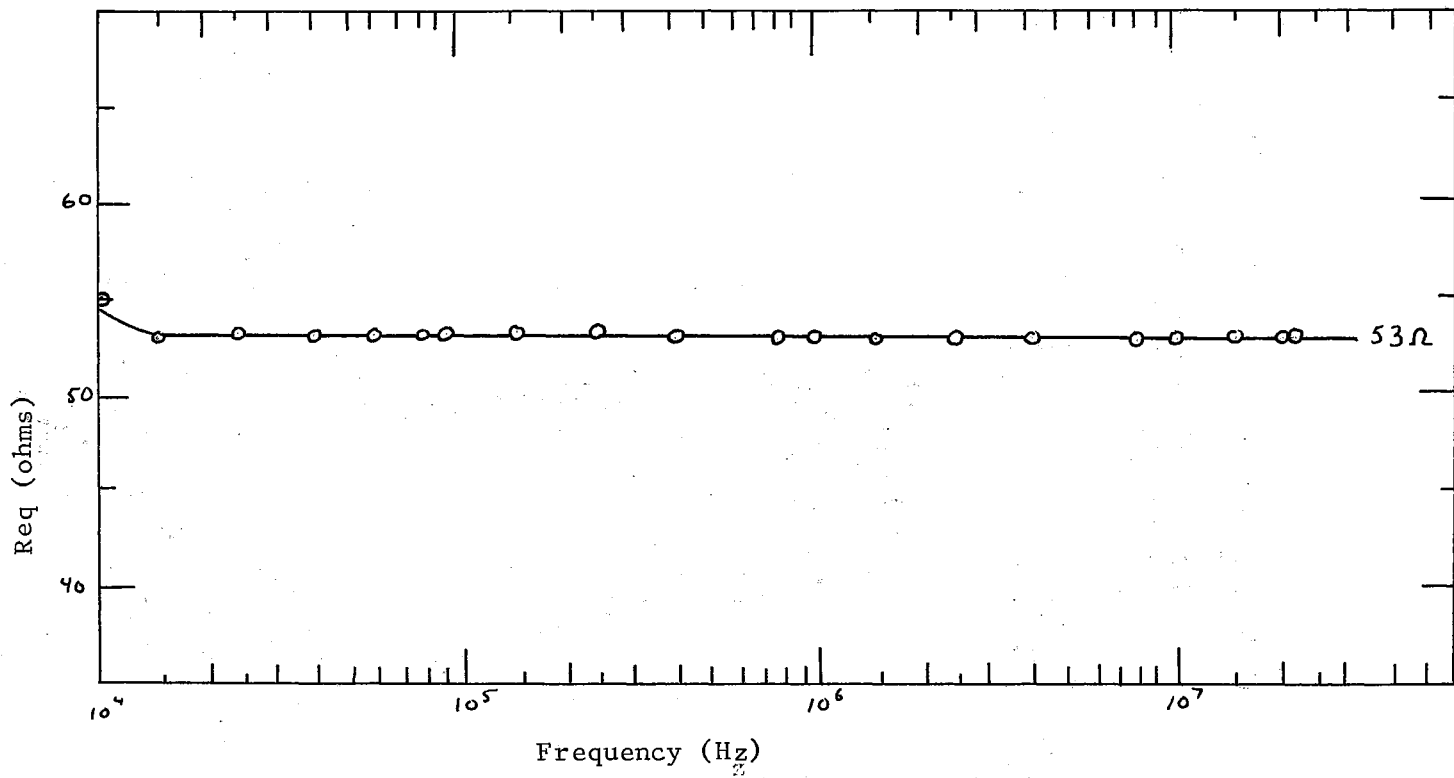


Figure 2. Equivalent Noise Resistance of the Preamplifier

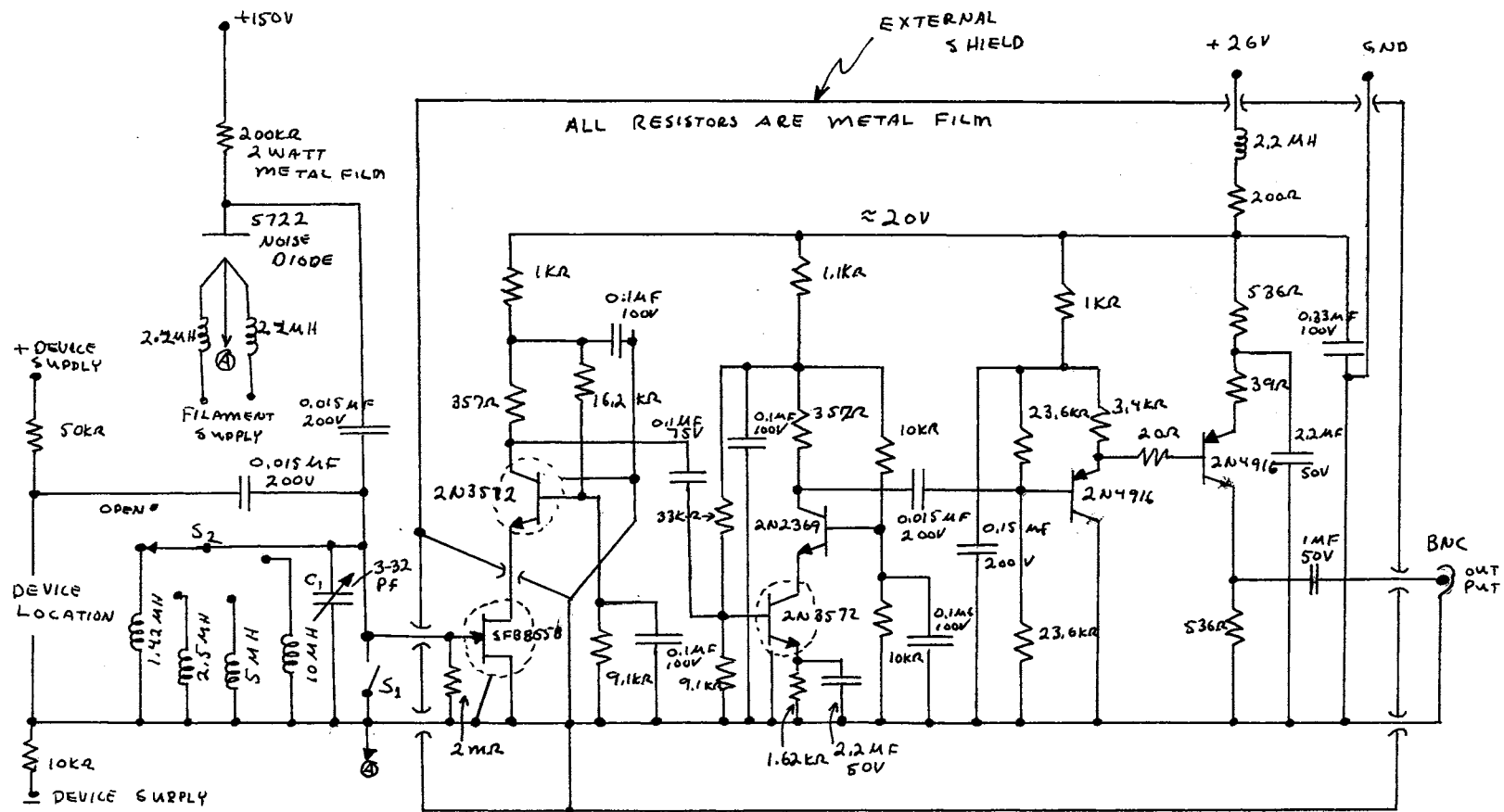


Figure 3. Preamplifier, Noise Calibration Tube, and DID Bias

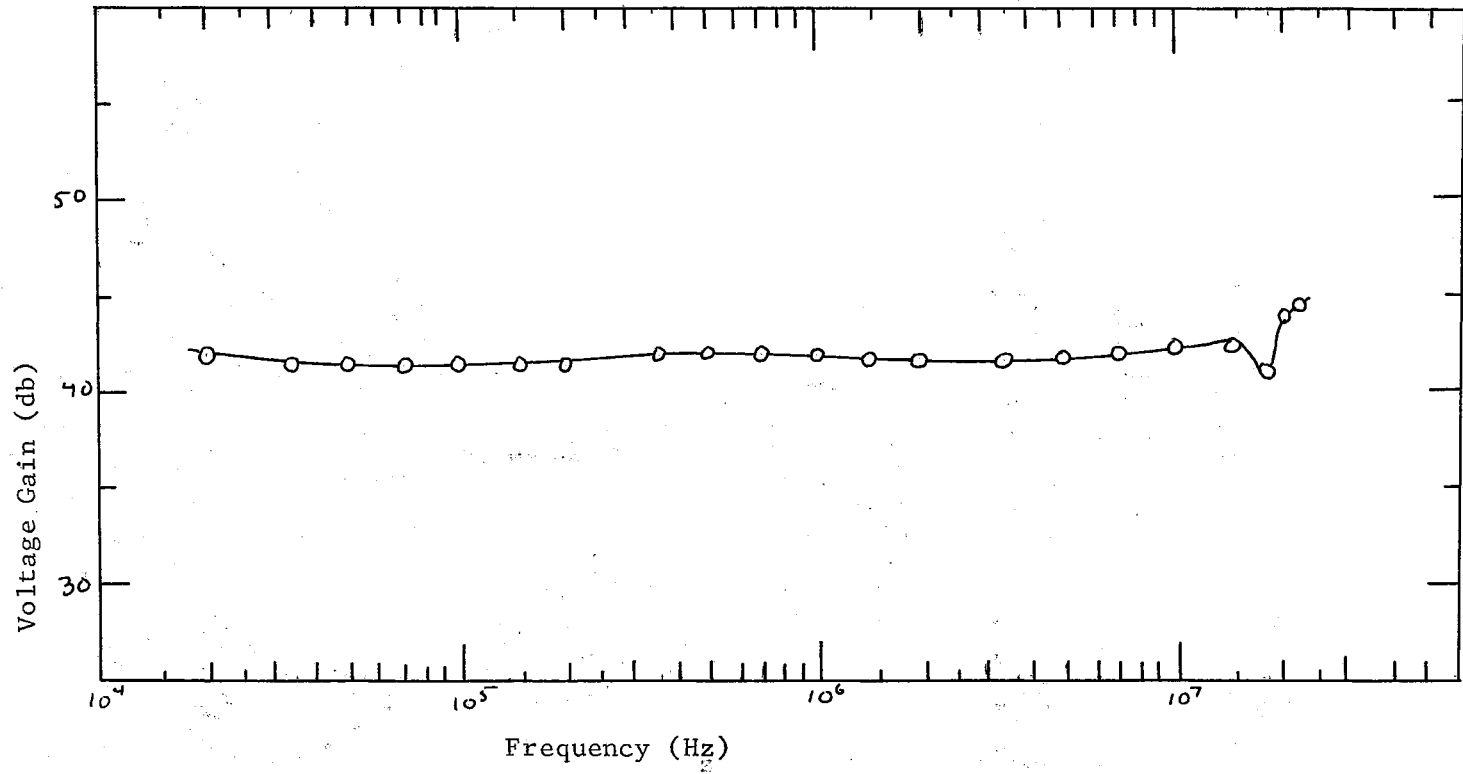


Figure 4. Voltage Gain in (db) of the Preamplifier vs. Frequency

Input Circuitry

The input circuitry consisted of the DID biasing resistors and coupling capacitor, the noise calibrator tube and its biasing resistors and coupling capacitor, the inductors L_1 , L_2 , L_3 , L_4 , switches S_1 and S_2 and the tuning capacitor C_1 . The biasing resistors for the DID and the noise tube isolate the power supplies from the input and establish a high impedance supply for both. S_1 is used to short the input and S_2 is used to select one of the four coils or no coil. The coils are used at high frequencies to null out the preamplifier input capacitance. The coils had to have a very high Q so the equivalent parallel resistance of the tuned circuit would be very large. This would allow noise measurements of high impedance devices. All of the coils had Q 's above 120 and were made by winding copper wire on lucite rods. The capacitance of the input circuitry was found to be 26 pF with minimum tuning capacitance. It was determined that four coils would be needed to cover a range from 7.5MHz to 22MHz with the measured input capacitance and the capacitance variation of C_1 .

Noise Calibration

The unknown noise of a device can be found by comparing the noise of the device to that added by a temperature-limited diode whose shot noise output is given by

$$\overline{I^2} = 2q I_c \Delta f \quad 2.6$$

where I_c is the D-C current flowing in the diode.

Worch (4) gives a relation for finding the equivalent noise current (I_{eq}) of an unknown device where this current is equal to the

current flowing in a temperature-limited diode whose noise output is the same as the unknown device

$$I_{eq} = \left[\frac{\overline{V_1^2} - \overline{V_s^2}}{\overline{V_2^2} - \overline{V_1^2}} \right] I_c - I_{eqz} \quad 2.7$$

where I_{eqz} is the equivalent noise current of the amplifier and the input circuitry with the device not connected to the input.

$$I_{eqz} = \left[\frac{\overline{V_1^2} - \overline{V_s^2}}{\overline{V_2^2} - \overline{V_1^2}} \right] I_c \quad 2.8$$

where

$(\overline{V_s^2})$ is the mean square shorted input amplifier noise and is related to the total noise of the amplifier;

$(\overline{V_1^2})$ is the mean square amplifier noise with the device at the input. This corresponds to the device noise and the amplifier noise;

$(\overline{V_2^2})$ is the mean square amplifier noise with a noise diode plate current I_c with the device at the input. This corresponds to the calibration source noise, the device noise and the amplifier noise.

The values of $\overline{V_s}$, $\overline{V_1}$, and $\overline{V_2}$ were read three times at each frequency and averaged for each of the conditions. First I_{eqz} is found with the device not connected to the input, then the measurements are redone with the device connected to the input so I_{eq} can be found.

CHAPTER III

EXPERIMENTAL RESULTS

This chapter presents the noise spectra of the silicon cube law DID. The noise spectra were measured for seven D-C bias conditions over a frequency range of 10KHz to 22MHz.

Background

A simple first order equivalent circuit was presented by Lee (2) for a double-injection diode and is shown in Figure 5.

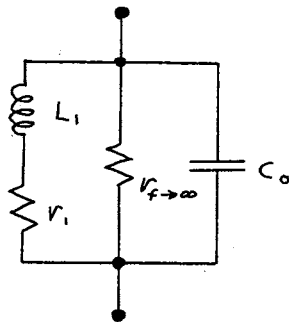


Figure 5. Equivalent Circuit for a DID

where $r_{f \rightarrow \infty}$ is the equivalent resistance of the DID at high frequencies, r_1 and L_1 are involved in generation-recombination noise and C_0 is the device capacitance.

Lee (2) also presented an expression for the equivalent noise current I_{eq}

$$I_{eq} = I_{eqth} + b/f^n \quad 3.1$$

where I_{eqth} is the equivalent thermal noise current and b/f^n is the frequency dependent component of the noise.

Results

The I-V characteristics of diode 2.8 is shown in Figure 6. The cube law region is above $100\mu A$ bias current for the device.

There were seven noise spectra measured for the diode for different D-C bias conditions ranging from a bias of $10\mu A$ to $4mA$ and a frequency range of $10KHz$ to $22MHz$. These noise spectra are shown in Figure 7. In all cases the equivalent noise current at high frequencies approached a flat asymptote. As the device current was increased, the noise asymptote also increased.

Computer Evaluation of the Data

A Least-Squares program was used to fit a curve of the form of Equation 3.1 to the measured data. This program printed the fitted points and the constants I_{eqth} , b , and n with the expected error associated with each constant. Because the thermal noise is the desired quantity, some of the low frequency points were dropped to improve the quality of the curve fit. Table I shows the fitted values of I_{eqth} , b and n for the different bias conditions. Figure 7 shows the fitted curve (solid lines) and the measured points.

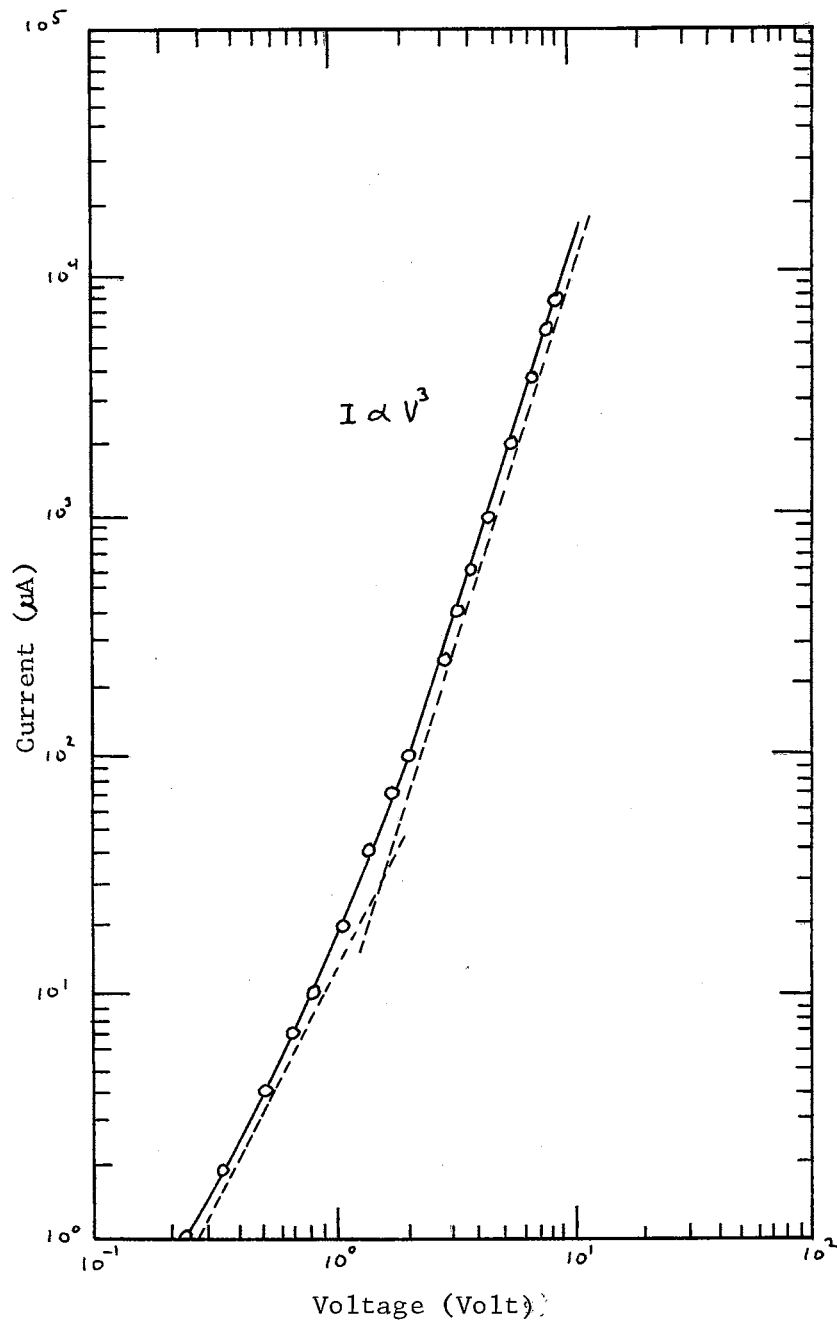


Figure 6. The I-V Characteristics of Diode 2.8

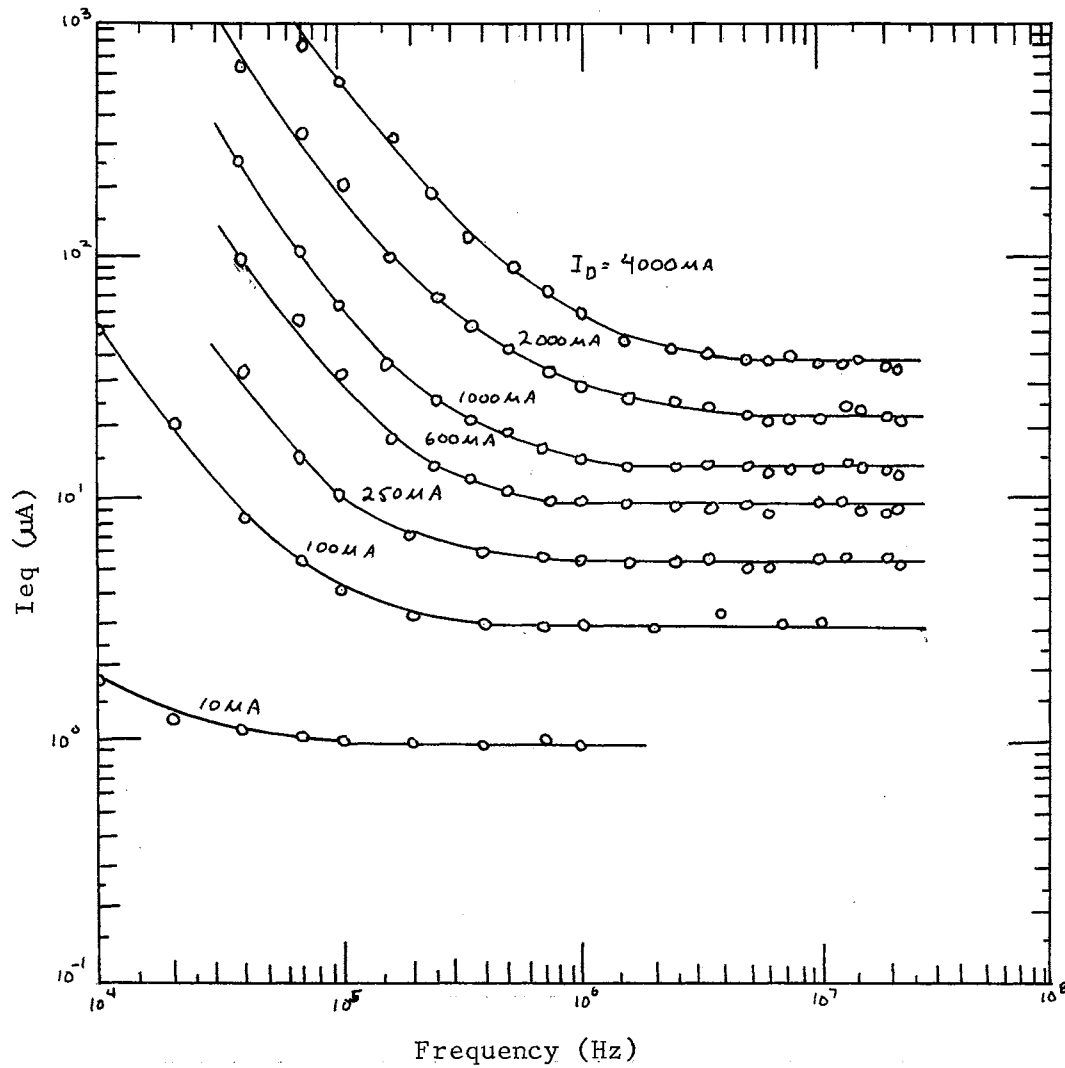


Figure 7. Measured Noise Spectra for Device 2.8

TABLE I
THE FITTED VALUES OF I_{eqth} , b AND n

Device Current (μA)	I_{eqth} (μA)	b	n
10	0.971 ± 0.007	0.0017 ± 0.0005	1.35 ± 0.06
100	3.00 ± 0.11	0.053 ± 0.006	1.47 ± 0.02
250	5.39 ± 0.06	0.117 ± 0.01	1.68 ± 0.03
600	9.39 ± 0.01	0.48 ± 0.06	1.65 ± 0.05
1000	13.7 ± 0.17	1.51 ± 0.18	1.54 ± 0.07
2000	22.7 ± 0.4	6.5 ± 0.6	1.41 ± 0.07
4000	36.6 ± 0.5	23.4 ± 0.95	1.34 ± 0.06

The equivalent noise current of a resistor R can be represented by

$$I_{eqR} = \frac{2KT}{qR} \quad 3.2$$

This relation can be derived by using the Norton equivalent of a noise source and the relation for shot noise.

Table II shows values of the device current, values of I_{eqth} that were extracted with the computer program, values of $r_{f \rightarrow \infty}$ from Bilger (5) and calculated values of $I_{eqR_{f \rightarrow \infty}}$.

TABLE II

 I_{eqth} AND $I_{eqr_{f \rightarrow \infty}}$ COMPARISON

Device Current (μA)	I_{eqth} (μA)	$r_{f \rightarrow \infty}$ ($k\Omega$)	$I_{eqr_{f \rightarrow \infty}}$ (μA) _o ($T=300^\circ K$)	$\left \frac{I_{eqth} - I_{eqr_{f \rightarrow \infty}}}{I_{eqth}} \right $
10	0.971 ± 0.007	54	0.96	0.0102
100	3.00 ± 0.11	18	2.88	0.04
250	5.39 ± 0.06	11	4.71	0.126
600	9.39 ± 0.01	6.5	7.97	0.151
1000	13.7 ± 0.17	4.2	12.3	0.102
2000	22.7 ± 0.4	2.6	19.9	0.123
4000	36.6 ± 0.5	1.5	34.5	0.0575

CHAPTER IV

ERROR ANALYSIS

With any experimental investigation there is a degree of uncertainty associated with the data. This uncertainty comes from errors which fall into three classes: statistical, calibration, and reading errors. Statistical errors are always present and must be taken into account. Calibration errors are from equipment inaccuracies and can sometimes be minimized, and they must be accounted for. Reading errors are human errors and can be reduced with patience on the part of the observer.

Statistical Errors

The form of statistical errors involved in the measurements was the relative standard error in the mean value of bandwidth limited white noise.

The relative standard error of a mean value measurement of bandwidth limited white noise comes from Bendat (6)

$$\alpha = (2 (\Delta f) t)^{-1/2} \quad 4.1$$

In applying this to the noise measurements, consider the equivalent noise current

$$I_{eq} = \left[\frac{\overline{V_1^2} - \overline{V_s^2}}{\overline{V_2^2} - \overline{V_1^2}} \right] I_c - I_{eqz} \quad 4.2$$

I_c remains relatively constant but $\overline{V_s}$, $\overline{V_1}$ and $\overline{V_2}$ are all fluctuating quantities measured on the same equipment with the same settings so their relative errors can be considered the same.

$$\frac{\overline{\Delta V_s}}{\overline{V_s}} = \frac{\overline{\Delta V_1}}{\overline{V_1}} = \frac{\overline{\Delta V_2}}{\overline{V_2}} = \alpha \quad 4.3$$

Assuming $\overline{V_s^2} \gg \overline{V_1^2}$ and $\overline{V_s^2} \gg \overline{V_2^2}$ and $I_{eq} \gg I_{eqz}$, it can be shown that

$$\frac{\overline{\Delta I_{eq}}}{I_{eq}} = 2 \sqrt{2} \alpha \quad 4.4$$

For $t = 5$ sec and $\Delta f = 3000$ Hz

$$\frac{\overline{\Delta I_{eq}}}{I_{eq}} = 1.66\% \quad 4.5$$

The total minimum expected statistical error is $\pm 1.66\%$ with these assumptions.

Equipment Errors

There must be a standard against which all equipment is calibrated. The standard used is a Dymec 2401B Integrating Digital Voltmeter which has a specified accuracy of $\pm 0.01\%$. It is assumed that the DVM is still within these specified accuracy limits.

Two Triplet 630NA meters were used as standards in the lab. The specified accuracy of these meters was $\pm 1.5\%$. Their accuracy was checked by passing a current through a known resistance ($5.0K\Omega \pm 0.05\%$) and monitoring the voltage drop of the resistor with the Dymec DVM. The two meters were found to have an accuracy within the specified limits of $\pm 1.5\%$.

The noise tube plate current meter was checked next with the two Triplet meters. Various values of plate currents were used and their

values recorded. These values were compared to the readings of the Triplet meters. The plate current meter always had a reading 0% to 4% higher than the Triplet meters's average with most of the readings being 1% higher than the Triplet reading. The total minimum error associated with the plate current of the noise diode will be the combined errors of the Triplet meters and the difference between the Triplet meters and the plate current meter. The total minimum error assigned to the plate current is +2.5% -0.5%. Any relative error in I_c will cause the same error in I_{eq} . (See Equation 2.7.)

The total minimum error assigned to the data is the sum of the statistical errors and the equipment errors. This total comes to a minimum error of +4.2% -2.2%.

Linearity Checks

Other forms of equipment errors include the possibilities of nonlinearities in the integrator or in the preamplifier output.

Integrator nonlinearities were checked for by applying a known D-C voltage to the input and recording the output voltage. Input voltages ranged from 0V to 1.0V (1 volt is the maximum output from the wave analyzer). The input and output voltages were recorded and the gain of the integrator was found. The values of the input, output and integrator gain are shown in Table III. Based on these values the integrator was considered linear.

TABLE III
INTEGRATOR GAIN

E_{source} (Volts)	E_{out} (Volts)	Gain $\frac{E_{\text{out}}}{E_{\text{source}}}$
0.101	9.79	96.9
0.201	19.61	97.6
0.301	29.39	97.6
0.401	39.23	97.8
0.507	49.67	98.0
0.608	59.53	97.9
0.707	69.23	97.9
0.801	78.34	97.8
0.909	89.04	98.0
0.987	96.60	97.9

The next step was to check the linearity of the preamplifier output. This was done by placing a known resistance at the preamplifier input and changing the noise tube bias current. Remember the squared noise current is proportional to the bias current I_c . If the source resistance was much larger than the equivalent noise resistance, then the output noise of the preamp would be proportional to the noise current, or $(V_{\text{out}})^2 \propto I_c$. Figure 8 shows V_m^2 vs I_c and was measured at a frequency of 1MHz. Figure 9 shows V_m^2 vs I_c measured at 22MHz. Here V_m is the wave analyzer reading. In both cases the plot was linear so it

can be assumed the preamp has a linear output. A 1,000 ohm resistor was used on the input in both cases.

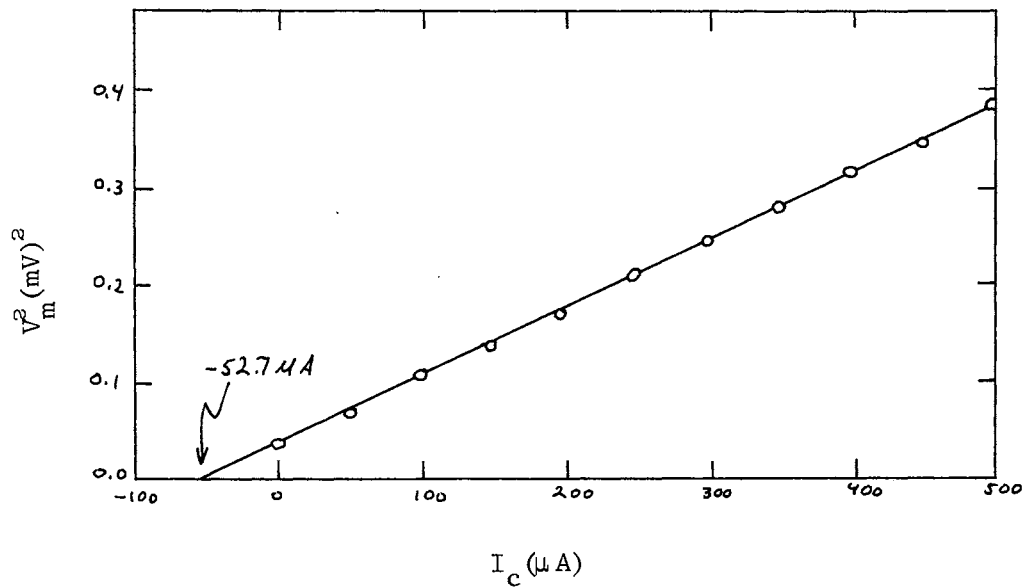


Figure 8. V_m^2 vs I_c at 1MHz

Resistor Calibration

Remember the thermal noise voltage of a resistor is given by

$$\overline{V^2} = 4KTR \Delta f \quad 4.6$$

Consider the Norton equivalent of the noise instead of the Thevenin equivalent and equate the noise powers.

$$\frac{\overline{V^2}}{R} = \overline{I^2} R = 4KT \Delta f \quad 4.7$$

Solving for $\overline{I^2}$ we find

$$\overline{I^2} = \frac{4KT \Delta f}{R} \quad 4.8$$

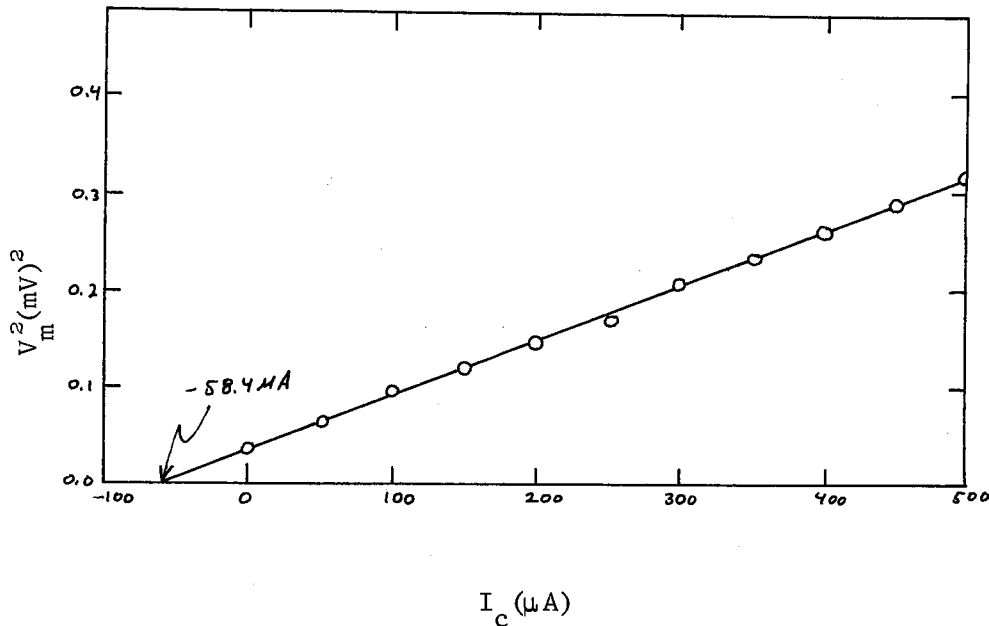


Figure 9. V_m^2 vs I_c at 22MHz

If the noise is considered like a shot noise source or

$$\overline{I^2} = 2q I_{eqR} \Delta f \quad 4.9$$

then the resistor's noise can be represented as an equivalent noise current. This can be found by equating equations 4.8 and 4.9 or

$$I_{eqR} = \frac{2KT}{qR} \quad 4.10$$

For $T = 300^\circ\text{K}$ and $R = 1000\Omega$

$$I_{eqR} = 51.69\mu\text{A} \quad 4.10a$$

This is very close to the $V_m^2 = 0$ crossing on the I_c axis of the output linearity checks. These values are higher than the expected values because of I_{eqz} associated with the input. A Linear Least-Squares program was used with the Hewlett-Packard 9100A desk computer to get the slope and the intercept points for Figures 8 and 9.

The theoretical equivalent noise current of a resistor can be found by equation 4.10. By letting a resistor be the unknown source, its measured value of I_{eqR} can be found by using equation 2.7. Figure 10 shows the noise spectra of three resistors 100 Ω , 1000 Ω and 10,000 Ω . The expected and measured I_{eqR} values are shown in Table IV.

TABLE IV
EXPECTED AND MEASURED VALUES OF I_{eqR}

R (ohms)	Calculated I_{eqR} (μ A)	Measured I_{eqR} (μ A)
100 \pm 1%	517.0	529
1,000 \pm 1%	51.70	54.5
10,000 \pm 1%	5.170	5.35

The measured values of I_{eqR} were the averages of the data points and in the three cases the measured values of I_{eqR} were not more than 5% higher than the calculated values of I_{eqR} .

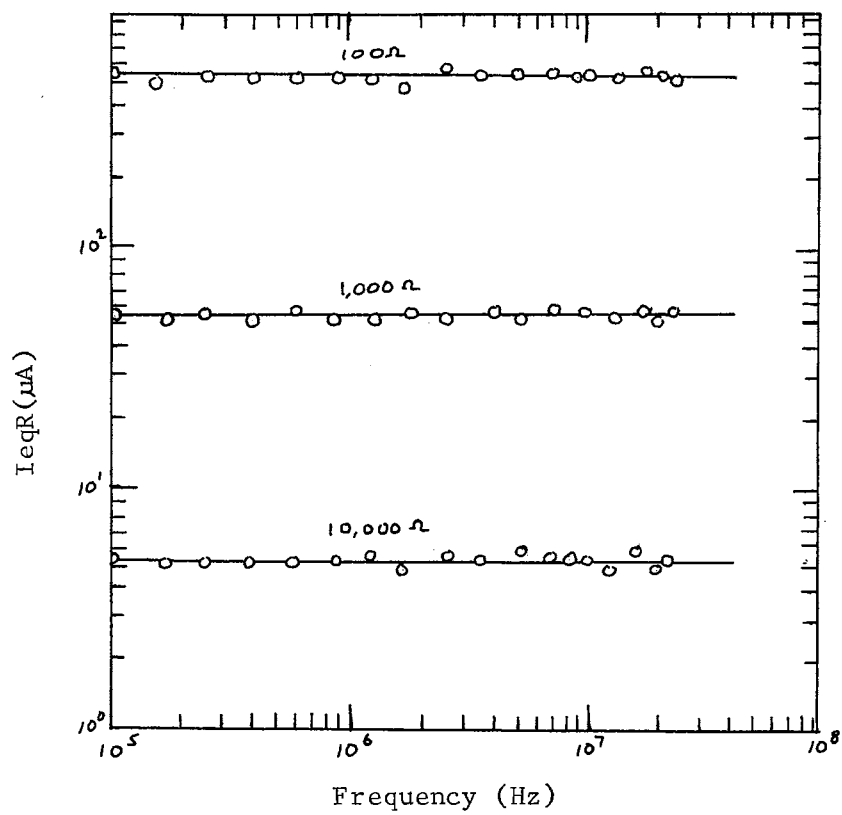


Figure 10. Noise Spectra for Three Resistors, 100Ω , $1,000 \Omega$ and $10,000 \Omega$

CHAPTER V

CONCLUSIONS

The noise spectra were observed to have a frequency-dependent component and a frequency-independent component (the thermal component). The thermal component of the noise was obtained by fitting a curve of the form

$$I_{eq} = I_{eqth} + b/f^n \quad 5.1$$

to the noise spectra. I_{eqth} is the thermal noise component and b/f^n is the frequency-dependent component of the noise.

The values of I_{eqth} that were obtained using the curve-fit program were compared to the calculated values of $I_{eqrf \rightarrow \infty}$. The values of $I_{eqrf \rightarrow \infty}$ were calculated by using Equation 4.10 and the measured values of $r_{f \rightarrow \infty}$ obtained from Bilger (5). The values of I_{eqth} did not differ by more than 15% of the $I_{eqrf \rightarrow \infty}$ values.

Recommendations for Further Study

Because there is only one device available at this time, noise studies of silicon cube-law devices are limited. Varying the ambient temperature, extending the frequency range of noise measurements and using D-C bias conditions that are higher and lower than what were used would provide additional information about thermal noise of double-injection diodes.

BIBLIOGRAPHY

- (1) Van der Ziel, A. Noise. New York: Prentice-Hall, 1954.
- (2) Lee, D. H. "Double Injection: High Frequency Noise and Temperature Dependence." (unpub. Ph. D. dissertation, California Institute of Technology, 1969).
- (3) Van der Ziel, A. "Thermal Noise in Field-Effect Transistors." Pro. IRE 1962, 1808-1812.
- (4) Worch, P. R. "An Experimental Investigation of Generation-Recombination Noise in Double-Injection Diodes." (unpub. Ph. D. dissertation, Oklahoma State University, 1970).
- (5) Bilger, H. R. Private communication.
- (6) Bendat, J. S. and A. G. Piersol. Measurement and Analysis of Random Data. New York: Wiley and Sons, 1966.

VITA

John Alan Maxwell

Candidate for Degree of

Master of Science

Thesis: AN EXPERIMENTAL INVESTIGATION OF THERMAL NOISE OF A SILICON
CUBE LAW DOUBLE-INJECTION DIODE

Major Field: Electrical Engineering

Biographical:

Personal Data: Born in Oklahoma City, Oklahoma, February 1, 1948,
the son of Mr. and Mrs. J. A. Maxwell.

Education: Graduated from Northwest Classen High School, Oklahoma
City, Oklahoma, in May, 1966; received the Bachelor of
Science in Electrical Engineering in January, 1971, from
Oklahoma State University; completed requirements for Master
of Science degree at Oklahoma State University in May,
1973.

Professional Experience: Summer Engineer Trainee, Schlumberger
Well Services, summers of 1969 and 1970; Associate Engineer,
Schlumberger Well Services, summer of 1972; Research
Assistant for the Electrical Engineering Department, Oklahoma
State University from June, 1971 to May, 1972.

Professional Organizations: Eta Kappa Nu, Institute of Electrical
and Electronic Engineers.